ISSN: 2157-7439
Journal of Nanomedicine & Nanotechnology

OPEN ACCESS Freely available online

Review Article

Periodontal Health Check by Nanoengineering Photoacoustic Imaging: Review

Casey Chen*

Department of Radiology, University of California, USA

ABSTRACT

The gold-standard periodontal probe is an outdated instrument that can diagnose periodontitis and track the condition of the gingiva, but it is also painful, prone to mistake, and does not completely characterise the periodontal pocket. These limitations can be overcome by a non-invasive method called photo acoustic imaging. Here, the periodontium was imaged using ultrasound frequencies between 16 and 40 MHz, and the pockets were identified using a cuttlefish ink-based contrast solution. The periodontal nano particles architecture, comprising the tooth, gum, gingival edge, and gingival thickness of teeth 7–10 and 22–27, could be spatially resolved using a 40 MHz ultrasound frequency. The measurements made using photo-acoustic-ultrasound were more accurate (0.01 mm) than those made using physical probes by a dental hygienist. Additionally, it was possible to see the complete geometry of the pockets using 10 percent relative standard deviations (n = 5). This work demonstrates the potential for photoacoustic-ultrasound imaging in the dental clinic for non-invasive monitoring of periodontal health. Nearly 50% of Americans have periodontitis, which has both local and systemic implications on the body. These include everything from little discomfort to incapacitating pain, tooth loss, and abnormal immune system activity.

Keywords: Inflammation; Dementia; Cardiovascular disease; Periodontitis

INTRODUCTION

In fact, studies have linked periodontitis' persistent inflammation to a number of diseases, including dementia, cancer, and cardiovascular disease. It is crucial to identify periodontal disease at an early stage, while the symptoms are manageable and reversible. Attachment level, probing depth, bone loss, mobility, recession, and degree of inflammation are some of the current criteria used to track periodontal health [1]. The evaluation of clinical attachment loss with a periodontal probe is the gold standard for determining the development of periodontitis. This tool offers a numerical measure of the strength of the apical epithelial attachment.

MATERIALS AND METHOD

It is crucial for disease staging and is assessed from the gingival border. The periodontal probe, on the other hand, is a low-tech instrument with poor reproducibility. These mistakes are a result of the large, between-operators difference in probing force, which can vary by many orders of magnitude. Physical probing can cause bleeding, patient discomfort, and erroneous measurements by penetrating inflammatory tissue. Additionally, the probe can only measure depth where it is inserted; it cannot determine the pocket's whole diameter or contour [2]. Additionally, the implant threads that prevent probe penetration along the implant surface negate the effectiveness of conventional probing around dental implants. This restricts clinical evaluation of these tissues that can cause peri implantitis. Recently, we discussed a method that might help with these problems using photo acoustic imaging. Photoacoustic imaging is a hybrid imaging technique that combines acoustic detection and visible and near-infrared excitation. Through the use of contrast based on optical absorption, it increases the usefulness of ultrasound. Photoacoustic imaging replaces the "sound in, sound out" tenet used in conventional ultrasonography with "light in, sound out" [3]. Here, a light-absorbing target is excited by a near infrared laser [fig 1]. The target is then heated within a small area before vascular malformations, non-invasive evaluation of Crohn's disease, and endogenous imaging of inflammatory arthritis. Despite the possibility of tissue penetration limiting photoacoustic-ultrasound (PA-US) signal, it has two key benefits over radiography, the most used dental imaging modality: it can image soft tissue, and it doesn't emit ionizing radiation. It is also possible to photograph the surfaces of hard tissues like bone and teeth. Hermoelastic expansion Wideband acoustic waves are produced as a result, and these waves can be detected by ultrasonic transducers to create images [4]. The therapeutic uses of photoacoustic imaging are expanding; some recent examples include endogenous imaging of

***Correspondence to:** Casey Chen, Department of Radiology, University of California, USA, E-mail: chen.casey@gmail.com

Received: 3-Aug -2022, Manuscript No: jnmnt-22-17873, **Editor assigned:** 6- Aug -2022, Pre QC No: jnmnt-22-17873 (PQ), **Reviewed:** 20- Aug -2022, QC No: jnmnt-22-17873, **Revised:** 23- Aug -2022, Manuscript No: jnmnt-22-17873 (R), **Published:** 30- Aug -2022, DOI: 10.35248/2157-7439.22.13.635.

Citation: Chen C (2022) Periodontal Health Check by Nanoengineering Photoacoustic Imaging: Review. J Nanomed Nanotech. 13: 635.

Copyright: ©2022 Chen C. This is an open-access article distributed under the terms of the Creative Commons Attribution License, which permits unrestricted use, distribution, and reproduction in any medium, provided the original author and source are credited.

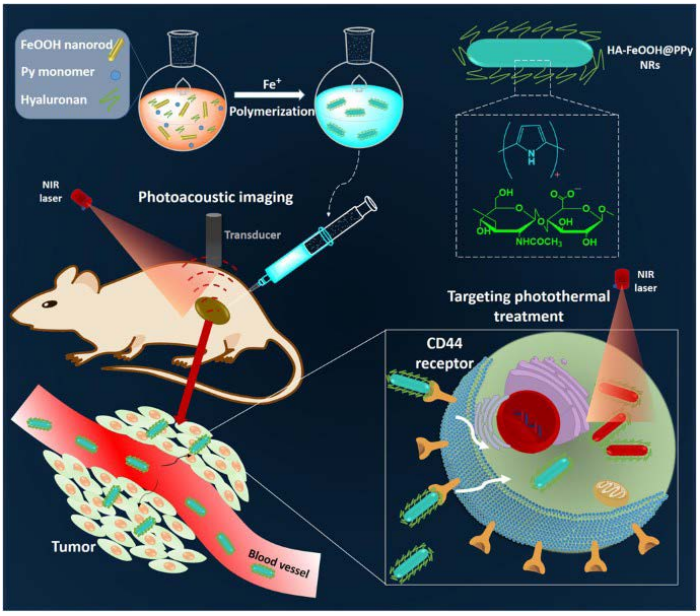

Figure 1: Nature Photoacoustic Imaging-Guided Photothermal Therapy.

inflammatory arthritis, non-invasive assessment of Crohn's disease, and identification of vascular abnormalities [5].

Our earlier study used a biocompatible oral contrast agent based on food-grade cuttlefish ink to demonstrate the first use of photoacoustics for periodontal health. In order to validate the procedure, that team photographed approximately 40 pig molars using swine models. Although the bias values compared to the gold standard were small (0.2 mm), there were still issues with the clinical applicability of the method. Here, we demonstrate that, following local irrigation of the pocket with contrast material, photoacoustic ultrasonography can imaging the complete depths and geometries of pockets in healthy adult human subjects [6]. Conservas de Cambados sold cuttlefish ink, which was made out of ink, water, salt, and sodium carboxymethyl cellulose.

RESULT

We bought phosphate-buffered saline tablets from Sigma-Aldrich. We bought ultrasound gel from Next Medical Products. Using Visualsonics laser-integrated high frequency ultrasound equipment, PA-US images were captured (Vevo LAZR). DealMed supplied a medical head immobiliser. We bought disposable dental cheek retractors from Url Dental. For each imaging experiment, unique contrast agent solutions were made using cuttlefish ink stock solutions. Stock cuttlefish ink solutions were aliquoted, then stored in the refrigerator at 50% w/v in 0.1 M PBS. A portion of the ink was diluted and combined with maize starch to create a final solution that contained 5% ink by volume and 2% corn starch to create the contrast agent [7]. It was heated for a moment to homogeneity is achieved by boiling. Before being used as a contrast agent, the spherical melanin nanoparticles were previously characterised by transmission electron microscopy, which revealed a mean particle size of 125 nm from 500 nanoparticles, and dynamic light scattering, which revealed a hydrodynamic radius of 266 nm with a Polydispersity index of 0.116. It is made of food-grade materials and has received institutional review board approval for usage in humans (IRB). A shellfish allergy or kosher diet were used as exclusion criteria for human subjects. A healthy 22-year-old adult female participant with good oral hygiene was included in this case study [8]. The UCSD IRB authorised every studies involving human participants, and the IRB's ethical guidelines as well as the 1975 Helsinki Declaration were followed. The participant provided written informed consent, and images were taken of teeth 7–10, 22–27.

DISCUSSION

A certified periodontist used the Williams and Marquis probes to measure pockets. According to clinical practise, the measurements were made at the distobuccal, mesiobuccal, and buccal locations [9]. The probe was inserted at a 10° angle at the interproximal gap between two teeth to take distal and mesial measurements. After walking the probe throughout the breadth of the pocket, the buccal measurements were taken at the deepest point that could be seen. Measuring was done in accordance with accepted clinical practise, rounding to the nearest integer. All measurements under 2 mm for the Williams probe were recorded as being 2 mm. Readings from the Marquis probe were rounded up to the closest millimetre after being estimated to be either in the lower 1.5 mm or above 1.5 mm range [10]. Eight litres of contrast agent were used to mark each sub gingival pocket. The gingival sulcus was in contact with a micropipette with a sterile 2-20 L tip, which was then utilised to irrigate the area with contrast agent. After imaging, the contrast agent was eliminated from the pockets by gently brushing the teeth or rinsing the mouth with water [11].

CONCLUSION

Pulsing light through two optical fibre bundles integrated with both sides of a rectangular, linear array transducer was used to accomplish photoacoustic imaging. 5 ns pulses at 20 Hz were used for the laser excitation (6 Hz frame rate). The three transducers LZ-201, LZ-250 (central frequency = 21 MHz), and LZ-550 (centre frequency = 40 MHz) were switched between to adjust the ultrasonic resolution. The typical gains for photoacoustic signals were 15 dB and 10 dB, respectively. During tests, both the subject and the operator wore near-infrared safety laser goggles. The individual placed their chin on a flat surface in front of the transducer while seated in front of the imaging system. To lessen motions that contribute to the condition, the subject wore dental cheek retractors and a medical head immobiliser. To artefacts in motion-based imaging. The transducer was covered with ultrasonic gel and positioned 1 cm away from the tooth. Maximum intensity projection was used to create a 3D PA-US image after the 680 nm laser was initialized and the stepper motor was scanned 17 mm (0.076 mm step size).

Sagittal cross-sections were examined in Image after raw data acquisition to gauge contrast agent penetration and calculate pocket depths [12]. Pictures were first transformed to 8-bit images and exported as two separate files, one of which only showed the photoacoustic signal and the other simply the ultrasound. A line profile was manually drawn through both of these photos, parallel to the gingival boundary. From there, the pixel intensity for both the photo-acoustic and the ultrasound pictures could be plotted with respect to the position along the line. The signal was then deemed significant when it exceeded a threshold of 4% minimum pixel intensity. When both signals at a specific location exceeded the threshold, that location was taken into consideration as a that of the pocket [13]. All of these points added up to a length, and its size was noted as the pocket depth. The first 8 sagittal planes (0.6 mm-wide sections) with a quantifiable pocket depth on each lateral side of the tooth were selected for distobuccal and mesiobuccal sites in order to prevent bias during quantitative comparison to physical probing. The diameters of these parts matched those of

the actual probes [14]. We chose 0.6 mm-wide slices from the pictures at the deepest point of the pocket for the buccal sites. This dimension replicated the physical probes' diameter and the common practise of taking the lowest number received by moving the probe over the pocket's width and recording it. Images are used for repeat measurements [15].

Acknowledgement

None

Conflict of Interest

None

REFERENCES

1. Shirvani H, Noori A, Mashayekh AM. The Effect of ZnO Nanoparticles on the Growth and Puberty of Newborn Male Wistar Rats. Int j sci basic appl res. 2014; 3: 180-185.
2. Yang Y, Qin Z, Zeng W, Yang T, Cao Y, Mei C. Toxicity assessment of nanoparticles in various systems and organs . Nanotechnol Rev. 2017; 6: 279-289.
3. Dhawan A, Sharma V. Toxicity assessment of nanomaterials: methods and challenges. Anal Bioanal Chem. 2010; 398: 589- 605.
4. Sano H, Hosokawa K, Kidoya H, Takakura N. Negative Regulation of VEGFInduced Vascular Leakage by Blockade of Angiotensin II Type 1 Receptor. Arterioscler Thromb Vasc Biol. 2006; 26: 2673-2680.
5. Ben-Slama I, Mrad I, Rihane N, Mir LE, Sakly M, Amara S. Sub-acute oral toxicity of zinc oxide nanoparticles in male rats. J Nanomed Nanotechnol. 2015; 6: 284-290.
6. Wang B, Feng W, Wang M. Acute toxicological impact of nano-and submicro-scaled zinc oxide powder on healthy adult mice. J Nanopart Res. 2008; 10 (2): 263–276.
7. Somayeh B, Mohammad F. Vitamin C can reduce toxic effect of nano zinc oxide. Int J Biological Sci. 2014; 3: 65-70.
8. Liu HL, Yang HL, Lin BC, Zhang W, Tian L, Zhang HS, et al. Toxic effect comparison of three typical sterilization nanoparticles on oxidative stress and immune inflammation response in rats. Toxicol Res. 2015; 4(2):486–493.
9. Espanani HR, Faghfoori Z, Izadpanah M, Babadi VY. Toxic effect of nano-zinc oxide. Bratisl Lek Listy. 2015; 116 (10): 616-620.
10. Elshama SS, Salem RR, Osman HEH, El-Kenawy AE. Toxic effect of sub-chronic use of zinc oxide nanoparticles on the lymphatic system of adult albino rats. Curr Top Toxicol J. 2017; 13: 127-137.
11. Fenech M. Micronuclei and their association with sperm abnormalities, infertility, pregnancy loss, pre-eclampsia and intra-uterine growth restriction in humans. Mutagenesis. 2011; 26: 63–67.
12. Tripathi R, Pancholi SS, Tripathi, P. Genotoxicity of ibuprofen in mouse bone marrow cells in vivo. Drug Chem Toxicol. 2012; 35 (4): 389–392.
13. Suzuki Y, Nagae Y, Li J, Sakaba H, Mozawa K, Takahashi A, et al. The micronucleus test and Erythropoiesis: effects of erythropoietin and a mutagen on the ratio of polychromatic to normochromatic erythrocytes (P/N ratio). Mutagenesis. 1989; 4(6):420-424.
14. Kirsch-Volders M, Vanhauwaert A, Eichenlaub-Ritter U, Decordier I. Indirect mechanisms of genotoxicity. Toxicol. Lett 2003; 140– 141: 63–74.
15. Tice RR , Agurell E, Anderson D, Burlinson B, Hartmann A, Kobayashi H, et al. Single cell gel/comet assay: Guidelines for in vitro and *in vivo* genetic toxicology testing. Environ Mol Mutagen. 2000; 35(3): 206-221.